 Cytometry Part A 67A:86–96 (2005)

# Novel Calibration Method for Flow Cytometric Fluorescence Resonance Energy Transfer Measurements Between Visible Fluorescent Proteins

**Peter Nagy,[1] László Bene,[1] William C. Hyun,[3] György Vereb,[1] Manuela Braun,[5] Christof Antz,[5] Jacques Paysan,[6] Sándor Damjanovich,[2] John W. Park,[4] and János Szöllősi[1,2]***

[1]Department of Biophysics and Cell Biology, Medical and Health Science Center, University of Debrecen, Debrecen, Hungary
[2]Cell Biophysical Work Group of the Hungarian Academy of Sciences, Research Center for Molecular Medicine, University of Debrecen, Debrecen, Hungary
[3]Cancer Center, University of California at San Francisco, San Francisco, California
[4]Department of Hematology/Oncology, University of California at San Francisco, San Francisco, California
[5]Otogene GmbH, Tübingen, Germany
[6]Institute of Zoology, Developmental Biology and Neurogenetics, Darmstadt University of Technology, Darmstadt, Germany

Received 11 January 2005; Revision Received 8 March 2005; Accepted 31 March 2005

**Background:** The combination of fluorescence resonance energy transfer (FRET) and flow cytometry offers a statistically firm approach to study protein associations. Fusing green fluorescent protein (GFP) to a studied protein usually does not disturb the normal function of a protein, but quantitation of FRET efficiency calculated between GFP derivatives poses a problem in flow cytometry.

**Methods:** We generated chimeras in which cyan fluorescent protein (CFP) was separated by amino acid linkers of different sizes from yellow fluorescent protein (YFP) and used them to calibrate the cell-by-cell flow cytometric FRET measurements carried out on two different dual-laser flow cytometers. Then, CFP-Kip1 was coexpressed in yeast cells with YFP and cyclin-dependent kinase-2 (Cdk2) and served as a positive control for FRET measurements, and CFP-Kip1 coexpressed with a random peptide fused to YFP was the negative control.

**Results:** We measured donor, direct, and sensitized acceptor fluorescence intensities and developed a novel way to calculate a factor ($\alpha$) that characterized the fluorescence intensity of acceptor molecules relative to the same number of excited donor molecules, which is essential for quantifying FRET efficiency. This was achieved by calculating FRET efficiency in two different ways and minimizing the squared difference between the two results by changing $\alpha$. Our method reliably detected the association of Cdk2 with its inhibitor, Kip1, whereas the nonspecific FRET efficiency between Cdk2 and a random peptide was negligible. We identified and sorted subpopulations of yeast cells showing interaction between the studied proteins.

**Conclusions:** We have described a straightforward novel calibration method to accurately quantitate FRET efficiency between GFP derivatives in flow cytometry.


**Key terms:** flow cytometry; fluorescence resonance energy transfer; green fluorescent protein

The conformation and association state of proteins are recognized as important factors in biological regulation. Fluorescence resonance energy transfer (FRET) is a physical phenomenon that can be used to measure in a quantitative way the average separation distance between two molecules (1). Although it was described in the 1940s by Dexter (2) and Förster (3), it has become a widely accepted biological research tool only in the past decade. In FRET, energy is transferred in a non-radiative fashion among an excited fluorescent molecule, the donor, and a nearby acceptor molecule that is usually, but not necessarily, fluorescent (4). Energy transfer efficiency (E) is

Contract grant sponsor: Hungarian Ministry of Health; Contract grant numbers: ETT524/2003; 532/2003; Contract grant sponsor: Hungarian Academy of Sciences; Contract grant numbers: OTKA T043061; F049025; T037831; Contract grant sponsor: European Union; Contract grant number: LSHB-CT-2004-503467; Contract grant sponsor: Fogarty International Collaboration Award; Contract grant number: 1 R02 TW00871-01A2; Contract grant sponsor: Békésy Fellowship, Hungarian Ministry of Education.

*Correspondence to: János Szöllsi, Department of Biophysics and Cell Biology, Medical and Health Science Center and Cell Biophysical Work Group of the Hungarian Academy of Sciences, Research Center for Molecular Medicine, University of Debrecen, Nagyerdei krt 98, 4012 Debrecen, Hungary.
E-mail: szollo@jaguar.unideb.hu

Published online 12 September 2005 in Wiley InterScience (www.interscience.wiley.com).
DOI: 10.1002/cyto.a.20164

defined as the fraction of excited donor molecules undergoing FRET and can be expressed in the following way:

$$E = \frac{R_0^6}{R_0^6 + R^6} \quad (1)$$

where R is the separation distance between the donor and the acceptor and $R_o$ is a distance at which E is 50%. $R_o$ is characteristic of a given donor-acceptor pair and its value is typically in the 3- to 8-nm range. The rate of FRET efficiency depends on the sixth power of the separation distance between the donor and the acceptor, thus providing a sensitive tool for the measurement of protein associations in the 2- to 10-nm range.

Before the introduction of green fluorescent protein (GFP) and its variants, which we collectively refer to as visible fluorescent proteins (VFPs), FRET measurements were limited to intrinsically fluorescent proteins or to proteins labeled with fluorescent ligands or antibodies. The advent of VFP-tagged proteins made FRET measurements in unperturbed systems much more widely applicable. Cyan and yellow fluorescent proteins (CFP-YFP) and blue fluorescent protein (BFP) and GFP are good donor-acceptor pairs based on their $R_o$ values and the overlap between donor and acceptor excitation and emission wavelengths (5). Many methods are available for the measurement of FRET. Several recent papers have been devoted for a comprehensive review of the topic (6–8), so we only briefly refer to flow cytometrically based FRET methods and to problems related to reliable quantification of FRET experiments.

In many cases, investigators have calculated FRET intensities or indices instead of reporting FRET efficiencies. FRET intensity is the fluorescence intensity measured in the FRET channel after correction for spectral overspill (9). It is sensitive for the amount of fluorophores expressed and thus is very error-prone. FRET indices are functions of the FRET efficiency only, but their interpretation is made difficult by the absence of a clear physical meaning of the calculated parameter (10). In addition, some of them may show interlaboratory variation. FRETN (11) and N-FRET (12) are FRET indices that take the donor and acceptor concentrations into account and are supposed to be true measurements of protein-protein interactions (11,12). Lately, their utility has been questioned based on their non-monotonous dependence on the acceptor concentration (13). Although methods based on the detection of increased donor anisotropy in the presence of FRET have a solid physical background, their results are difficult to interpret in terms of protein associations without resorting to complicated modeling (14–16).

A plethora of approaches exists that yields the FRET efficiency itself. We previously reported one such method based on the combined detection of donor and acceptor fluorescence intensities in cells labeled with fluorescent ligands or antibodies using flow cytometry (17,18). Later, we established a similar method in fluorescence microscopy (19). These methods require a factor, variably called $\alpha$ (17–19) or G (11,13), which relates the intensity lost on the donor side due to donor quenching to the enhanced emission of the acceptor due to sensitized emission. Methods for the determination of $\alpha$ have been reported for antibody-labeled cells in flow cytometry (17,18) and microscopy (19) and lately for VFP-expressing cells in microscopy (13). To the best of our knowledge, successful determination of $\alpha$ has not been reported for VFP-expressing cells using flow cytometry. A popular approach for the determination of FRET efficiency is based on the release of donor quenching upon photodestruction of the acceptor (20,21). Although this method has been applied to conventional fluorophores (20) and VFP-expressing cells (21), it cannot be used in flow cytometry because detection of donor fluorescence intensity before and after acceptor photobleaching is usually not feasible.

Because flow cytometry is statistically superior to fluorescence microscopy, it is an attractive method for FRET measurements. As discussed above, accurate determination of the FRET efficiency in VFP-expressing cells has not been accomplished in flow cytometry. We present such an approach, and its novelty lies in the determination of $\alpha$ in cells expressing VFP using flow cytometry. We demonstrate the reliability of the approach using cells with and without interaction between the donor and acceptor VFP derivatives.

## MATERIALS AND METHODS

### Cells

*Saccharomyces cerevisiae* INV Sc1 cells with the auxotroph markers trp1, ura3, leu2, and his3 were used. Cells were transformed using polyethylene-glycol/lithium acetate and heat shock (42°C for 15 min) and then plated on glucose-containing selection plates. pYES2- and pYES3-based constructs complemented for the ura3 and trp1 auxotroph markers, respectively. To induce protein expression under the control of the GAL1 promoter in pYES2 or pYES3, 2- to 3-day-old colonies were transferred to galactose/raffinose-containing plates, and VFP expression was checked every hour with a fluorescence microscope. Best expression results were obtained 6 to 8 h after induction.

### Plasmids

A detailed description of the cloning strategy has been published elsewhere (22); therefore we give a brief summary only.

**Cloning of VFP variants.** GFP (GFP-S65G-S72A) *mut-3* optimized for codon usage in the yeast (yGFP) (23) was provided in a pUC19 vector by Dr. Alistair J. P. Brown (Institute of Medical Science, University of Aberdeen). To make purification of the expressed proteins easier, a hexa-His tag was added to the N-terminus of yGFP using polymerase chain reaction (PCR). Because every construct was derived from yGFP, all contained the hexa-His tag. One additional mutation was introduced (T203Y) to convert yGFP to yYFP. Six mutations (F64L, S65T, Y66W, N146I, M153T, V163A, and N212K) were needed to generate yCFP from yGFP. In addition to the spectral shift, these mutations increased water solubility, temperature resistance, and maturation rate of the protein (24–29). yYFP and yCFP were cut out of pUC19 with *Hind*III and *Eco*RI

and cloned into pYES2 (Invitrogen, Karlsruhe, Germany) using the same restriction sites.

**Cloning of the CFP-30Pro-YFP construct.** Synthetic oligonucleotides (Gibco-Invitrogen, Karlsruhe, Germany) coding for 30 prolines with *Eco*RI/*Bam*HI sticky ends (forward: AATTC CCA CCA CCT CCA CCA CCT CCA CCA CCC CCA CCA CCT CCA CCA CCT CCA CCA CCC CCA CCA CCT CCA CCA CCT CCA CCA CCC CCA CCA CCT G; reverse: GATCC AGG TGG TGG GGG TGG TGG AGG TGG TGG AGG TGG TGG GGG TGG TGG AGG TGG TGG AGG TGG TGG GGG TGG TGG AGG TGG TGG AGG TGG TGG G) were annealed and ligated into a modified pGAD T7 vector (Clontech, Palo Alto, CA, USA) in which the *Hind*III restriction site at position 2280 was destroyed. A *Hind*III/*Eco*RI fragment of pUC19 containing yECFP was cloned in front of the linker. Then the yCFP+30 Pro segment was cut out with *Hind*III/*Bam*HI and ligated into pYES2 into which yYFP had already been cloned.

**Cloning of the CFP-3Gly-YFP construct.** Three glycine (Gly) residues were added to the C-terminus (3′ end) of yCFP by PCR, and the yCFP+3 Gly segment was inserted into pYES2-yYFP via *Hind*III/*Bam*HI 5′ of yYFP.

**Cloning of the CFP-25 AA-YFP construct.** The donor and the acceptor were linked by the trypsin-sensitive linker SSMTGGQQMGRDLYDDDDKDPPAEF (26) using two PCR steps. First, yYFP-containing pUC19 was used as a template and the sequence GRDLYDDDDKDPPAEF was added to the 5′ end of yYFP and a *Pst*I site to the 3′ end. Then this PCR product was used as a template and an *Eco*RI restriction site and the rest of the linker (SSMTGGQQM) was added to the 5′ end. The final PCR product was cloned into yCFP-containing pUC19 via *Eco*RI/*Pst*I 3′ of yCFP and cut out of pUC19 via *Hind*III/*Xba*I and cloned into pYES2.

**Cloning of CFP-Kip1 and YFP plus cyclin-dependent kinase-2.** Kip1 (accession no. U10906, with V109G mutation) and cyclin-dependent kinase-2 (Cdk2; accession no. X61622, with S177C mutation) were provided by Otogene USA (Seattle, WA, USA), cut out of pGAD T7 with *Eco*RI/*Xho*I, and inserted in-frame to the 3′ end of the yCFP-containing pYES2 plasmid or the yYFP-containing pYES3 plasmid using the above restriction sites.

### Purification of His-Tagged CFP-YFP Constructs

Yeast cells were grown on selective plates without galactose. A preculture was prepared in 5 ml of basic drop-out medium without galactose. The main culture was started at an $OD_{600}$ of 0.2 and grown overnight until an $OD_{600}$ of ~2 was reached. Protein expression from the GAL1 promoter was induced by 2% galactose for 6 h. Cells were pelleted, resuspended in breaking buffer (11.3 mM $NaH_2PO_4$, 38.7 mM $Na_2HPO_4$, pH 7.4, 1 mM ethylenediaminetetraacetic acid, 5% glycerol, 1 mM phenyl methyl sulfonyl fluoride), and lysed using glass beads (G8772, Sigma, Budapest, Hungary). His-tagged proteins were purified from the cell lysate on an Äkta Basic high-performance liquid chromatographic system using HisTrap HP columns (Amersham Biosciences, Freiburg, Germany).

### Flow Cytometry

A modified Becton-Dickinson Facstar Plus flow cytometer was used for energy transfer measurements. The 457- and 514-nm lines of two argon ion lasers were used to excite CFP and YFP, respectively. Donor and acceptor emissions were separated by a 525-nm dichroic mirror and were detected through 487/37-nm and 560/70-nm bandpass mirrors, respectively. Donor, acceptor, and FRET intensities were recorded as described previously (17,18). Briefly, two fluorescence intensities were detected for the donor excitation at 457 nm (donor channel $I_1$, detection at 487 nm; acceptor channel $I_2$, emission corresponding to the FRET channel at 560 nm), and one intensity was measured for the acceptor excitation at 514 nm ($I_3$, acceptor emission at 560 nm). For experiments with BFP and GFP, the ultraviolet lines (334 to 364 nm) and the 488-nm line of two argon ion lasers were used. BFP and GFP fluorescence emissions were separated by a 495-nm dichroic mirror and detected through 440/50-nm and 525/50-nm bandpass filters, respectively. Two fluorescence intensities ($I_1$, $I_2$) and one fluorescence intensity ($I_3$) were recorded from the intersection points corresponding to the donor and acceptor excitations, respectively, as described above.

In other experiments a Becton-Dickinson FACSVantage flow cytometer was used to measure FRET between CFP and YFP. CFP and YFP were excited by argon-krypton and argon ion lasers at 406 to 415 nm and 514 nm, respectively. The emitted fluorescence was collimated and photons originating from the two laser lines were separated by a half-mirror that reflected only the beam coming from the 406- to 415-nm excitation. This reflected beam was further divided by a 510-nm dichroic mirror, and donor and acceptor fluorescence intensities were measured through 450/50-nm and 560/70-nm bandpass filters, respectively, corresponding to $I_1$ and $I_2$. The beam from the 514-nm excitation was measured through a 575/26-nm bandpass filter ($I_3$).

### Mathematical Background of Flow Cytometric FRET Calculations

There are three unknowns in an experimental system in which the interaction of a protein pair separately labeled with donor and acceptor is investigated: the densities or amounts of the donor and acceptor and the FRET efficiency. Therefore, three independent measurements have to be taken that correspond to the donor ($I_1$), FRET ($I_2$), and acceptor ($I_3$) channels (17,18):

$$I_1(\lambda_{D,ex}, \lambda_{D,em}) = I_D(1 - E) \quad (2)$$

$$I_2(\lambda_{D,ex}, \lambda_{A,em}) = I_D(1 - E)S_1 + I_A S_2 + I_D E\alpha \quad (3)$$

$$I_3(\lambda_{A,ex}, \lambda_{A,em}) = I_D(1 - E)S_3 + I_A + I_D E\alpha \frac{S_3}{S_1} \quad (4)$$

Subscripts D and A refer to donor and acceptor, respectively, and subscripts ex and em stand for excitation and emission, respectively. $I_D$ and $I_A$ are the unquenched

donor and direct acceptor intensities, respectively; and E represents FRET efficiency. The constants $S_1$ to $S_3$ correct for the spectral overspill between the detection channels. $S_1$ corrects for the overspill of donor fluorescence from $I_1$ to $I_2$, $S_3$ for the overspill of donor fluorescence from $I_1$ to $I_3$, and $S_2$ for the overspill of acceptor emission from $I_3$ to $I_2$. The constants $S_1$ to $S_3$ are determined on single-labeled samples as described previously (17,18) and can be expressed by the following equations:

$$S_1 = \frac{\eta_D(I_2)}{\eta_D(I_1)} \tag{5}$$

$$S_2 = \frac{\rho(\lambda_{D,ex})\varepsilon_A(\lambda_{D,ex})\eta_A(I_2)}{\rho(\lambda_{A,ex})\varepsilon_A(\lambda_{A,ex})\eta_A(I_3)} \tag{6}$$

$$S_3 = \frac{\rho(\lambda_{A,ex})\varepsilon_D(\lambda_{A,ex})\eta_D(I_3)}{\rho(\lambda_{D,ex})\varepsilon_D(\lambda_{D,ex})\eta_D(I_1)} \tag{7}$$

where $\eta_D(I_x)$ and $\eta_A(I_x)$ represent the detection efficiencies of donor and acceptor fluorescences, respectively, in the $I_x$ fluorescence channel; $\rho(\lambda_{D,ex})$ and $\rho(\lambda_{A,ex})$ denote the photon fluxes of the lasers used for donor and acceptor excitation, respectively; $\varepsilon_D$ and $\varepsilon_A$ refer to the molar absorption coefficients of the donor and acceptor, respectively, at the wavelengths in parentheses. $\eta_A(I_2)$ and $\eta_A(I_3)$ are equal if the same detector is used for the measurement of $I_2$ and $I_3$.

It can be seen from equations 2 to 7 that the constant $\alpha$ is necessary for the calculation of FRET efficiency on a cell-by-cell basis. The $\alpha$ value relates the fluorescence intensity of acceptors in detection channel $I_2$ to the intensity of the same number of excited donor molecules in detection channel $I_1$ and can be expressed according to the following equation:

$$\alpha = \frac{\Phi_A\eta_A(I_2)}{\Phi_D\eta_D(I_1)} \tag{8}$$

where $\Phi_D$ and $\Phi_A$ represent the fluorescence quantum efficiencies of the donor and acceptor, respectively. For determination of $\alpha$ in flow cytometry, two samples with an equal number of donor and acceptor molecules are needed. Alternatively, one sample expressing the same number of non-interacting (E = 0%) donor and acceptor molecules is necessary. Such samples are very difficult to prepare, so an alternative approach had to be developed.

## RESULTS

### Theory of Determining α and the Absorption Ratio

We used two different methods to calculate FRET from flow cytometric data. According to the method involving $\alpha$ as described in Materials and Methods, FRET can be calculated from equations 2 to 4:

$$\frac{E}{1-E} = \frac{1}{\alpha}\left(\frac{I_2 - S_2I_3}{\left(1-\frac{S_2S_3}{S_1}\right)I_1} - S_1\right) = \frac{1}{\alpha}R_1 \tag{9}$$

$$E = \frac{R_1}{\alpha + R_1} \tag{10}$$

FRET calculation can alternatively be based on the following equation:

$$\frac{F_{AD}}{F_A} = 1 + \frac{\varepsilon_D c_D}{\varepsilon_A c_A}E = R_F \tag{11}$$

where $F_{AD}$ and $F_A$ are the fluorescence intensities of the acceptor in the presence and absence of the donor, respectively; and $c_D$ and $c_A$ are the molar concentrations of the donor and acceptor, respectively. $F_{AD}$ and $F_A$ can be expressed according to the notation of equations 2 to 4:

$$F_{AD} = I_2 - I_1S_1 \tag{12}$$

$$F_A = I_AS_2 \approx I_3S_2 \tag{13}$$

The above approximation holds if $S_3$ is negligible and $S_1 > S_3$. In our case, $S_3 < 0.01$ and $S_1 > 1$; therefore, neglecting the terms containing $S_3$ in equation 4 is substantiated. FRET efficiency can be isolated from equation 11:

$$E = \frac{R_F - 1}{\frac{\varepsilon_D c_D}{\varepsilon_A c_A}} \tag{14}$$

The drawback of the first approach (equation 10) is that it involves $\alpha$, and the disadvantage of the second method (equation 14) is that it involves the absorption ratio $(\varepsilon_D c_D)/(\varepsilon_A c_A)$, a parameter also difficult to determine experimentally in flow cytometry. If there are a series of samples with different FRET efficiencies in which the donor and the acceptor are expressed in a 1:1 ratio, one of these samples is selected as a reference (displayed with index 1), and the FRET efficiencies of the rest of the samples are divided by the FRET efficiency of the reference sample eliminating the absorption ratio. These ratios are separately calculated according to methods 1 (equation 10) and 2 (equation 14); their difference is calculated and summed for all the samples:

$$\sum_{j=2,3..n}\left(\frac{R_{F,1}-1}{R_{F,j}-1} - \frac{R_{I,1}}{\alpha + R_{I,1}}\frac{\alpha + R_{I,j}}{R_{I,j}}\right)^2 \tag{15}$$

The fact that the donor and the acceptor are expressed in a 1:1 ratio eliminates the donor and acceptor concentrations from equation 15, the minimum of which is found by changing $\alpha$ to yield $\alpha$ itself, because the two approaches are expected to give identical FRET efficiencies. A 1:1 donor:acceptor ratio is not required for this method, but a constant

Table 1
*Calibration of FRET Values Using the Three CFP-YFP Constructs*[*]

| | $I_1$ | $I_2$ | $I_3$ | $R_I$ | $R_F$ | FRET (%) From $R_I$ | FRET (%) From $R_F$ | $I_D$ | $I_A$ | $\varepsilon_D/\varepsilon_A$ |
|---|---|---|---|---|---|---|---|---|---|---|
| 30 Pro | 143 | 425 | 225 | 0.62 | 1.54 | 9.8 | 10.1 | 158 | 224 | 5.9 |
| 25 AA | 179 | 615 | 297 | 1.05 | 1.87 | 15.6 | 16.3 | 210 | 296 | 6.0 |
| 3 Gly | 109 | 586 | 233 | 2.82 | 2.79 | 33.1 | 33.5 | 159 | 231 | 5.8 |

[*]Fluorescence intensities in the donor, FRET, and acceptor channels were measured. Autofluorescence-corrected values are presented in columns $I_1$ to $I_3$. $R_I$ and $R_F$ values calculated from flow cytometric data and the FRET values derived from these ratios according to equations 10 and 14 are presented. The $\alpha$ value and the absorption ratio ($\varepsilon_D/\varepsilon_A$) were calculated from $R_I$ and $R_F$ and were 5.7 and 5.3, respectively. $I_D$ and $I_A$ values were determined by solving equations 2 to 4 using the constants $S_1 = 1.31$, $S_2 = 0.68$, and $S_3 = 0.004$, and the absorption ratio was determined according to equation 18 for every sample.

donor:acceptor ratio in every sample is necessary. We opted for a 1:1 ratio because this seemed to be the easiest to accomplish. If $F_{AD}/F_A$ calculated according to equations 12 and 13 is plotted against E calculated according to equation 10 using $\alpha$ derived as described above, the slope of the graph yields the absorption ratio (see equation 11).

By substituting equation 10 into equation 11 the relationship between $R_F$ and $R_I$ can be determined:

$$R_F = 1 + \frac{\varepsilon_D c_D}{\varepsilon_A c_A}\frac{R_I}{\alpha + R_I} \tag{16}$$

The linear form of equation 16 can also be used to derive the absorption ratio and $\alpha$:

$$\frac{1}{R_F - 1} = \frac{\varepsilon_A c_A}{\varepsilon_D c_D}\left(1 + \frac{\alpha}{R_I}\right) \tag{17}$$

A plot of $1/(R_F - 1)$ against $1/R_I$ yields a line with an intercept of $(\varepsilon_A c_A)/(\varepsilon_D c_D)$ and a slope of $\alpha \times$ intercept. Similar to the above described minimization approach, the linear regression also provides the absorption ratio and $\alpha$.

If the donor and the acceptor are expressed in a 1:1 ratio and $\alpha$ is known after minimizing equation 15, the unquenched donor ($I_D$) and direct acceptor ($I_A$) intensities can be calculated by solving the set of equations 2 to 4 (18). The only compensation necessary to get the fluorescence intensities of an equal number of donor and acceptor molecules is the correction for the different molar extinction coefficients of the donor and the acceptor, because the same laser line is used for the donor ($I_1$) and FRET ($I_2$) channels. Therefore, $\alpha$ can be calculated according to the following equation:

$$\alpha = \frac{I_A S_2}{I_D}\frac{\varepsilon_D(\lambda_D)}{\varepsilon_A(\lambda_D)} \tag{18}$$

The absorption ratio can be easily calculated from equation 18.

## Determining α and the Absorption Ratio Using Three CFP-YFP Constructs

We generated three CFP-YFP chimeras in which the fluorophores were separated by three glycines, 30 prolines, or a trypsin-sensitive linker consisting of 25 amino acids (26), and the proteins were expressed in yeast cells. The $\alpha$ value was determined by minimizing equation 15, and the absorption ratio was calculated from the slope plotted according to equation 11. The absorption ratio was also calculated for each sample by using equation 18. In addition, the absorption ratio and $\alpha$ were determined according to equation 17 in one step. The calculations yielded similar results (Table 1, Fig. 1). FRET efficiencies were calculated according to equations 10 and 14 (Table 1, Fig. 2). In addition, the FRET efficiency of the CFP-YFP construct in which the fluorophores were separated by the trypsin-cleavable linker were determined by trypsin-induced de-quenching (26), yielding a FRET efficiency of 20%, a value very close to our flow cytometric results. FRET calculated by the two flow cytometric methods are identical within experimental error, and their magnitude changes as expected: the FRET efficiency of the CFP-3Gly-YFP sample is the highest, followed by the CFP-25AA-YFP and CFP-30Pro-YFP samples. The 30-Pro linker is thought to form a rigid helix between CFP and YFP (see Discussion for more details), and the 25-AA and 3-Gly linkers maintain a shorter separation distance according to the length of their amino acid chains. A similar series of BFP-GFP chimeras were also generated. Unfortunately, we could not carry out a reliable determination of $\alpha$ using this FRET pair for reasons presented in the Discussion.

## Reliability of the Determination of α

The mean squared error (MSE) of the minimized norm can be determined according to the following equation:

$$MSE = \frac{\sum_{j=2,3..n}\left(\frac{R_{F,1} - 1}{R_{F,j} - 1} - \frac{R_{I,1}}{\alpha + R_{I,1}}\frac{\alpha + R_{I,j}}{R_{I,j}}\right)^2}{n - 1} \tag{19}$$

The MSE was calculated from the data presented in Table 1, and it is shown in Figure 3A. In a separate experiment, $\alpha$,

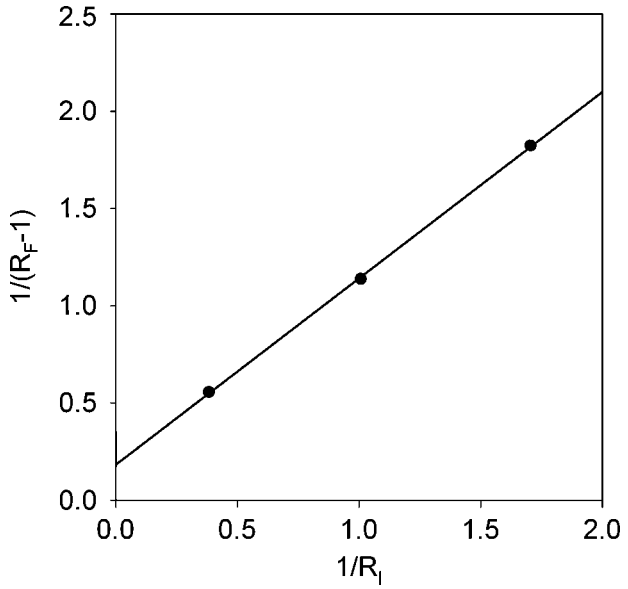


FIG. 1. Determination of α and the absorption ratio using linear regression. $R_F$-$R_I$ pairs measured on the three calibration samples were plotted according to equation 17, and a line was fitted, yielding a slope of 0.96 and an intercept of 0.18. From these values the absorption ratio and α were determined to be 5.48 and 5.26, respectively.

the absorption ratio, and the FRET efficiencies were determined using different optical alignment and detector settings. The α value was much smaller (0.615 instead of 5.7), and the MSE increased much faster around the minimum, especially in the case of large α values (Fig. 3B). Noisy measurements can give rise to weak dependence of MSE on α, leading to unreliable determination of the minimum. Therefore, we investigated whether the significantly different shape of the MSE(α) curve is related to noise or to the different values of α determined by the experimental setup. A computer simulation was carried out assuming an absorption ratio of 5 and FRET efficiencies of 5%, 15%, and 30% for the calibration samples. $R_F$ values were calculated from equation 14, and $R_I$ values were determined according to equation 10 using four different α values (0.5, 2, 5, and 10). The MSE was then calculated using equation 19 (Fig. 3C). It can be seen that the MSE increases much faster around the minimum if α is small. We concluded that the different dependences of the MSE on α shown in Figures 3A and 3B are at least partly caused by optical and other instrumental factors unrelated to noise.

### Confidence Interval of α

Given the weak dependence of the MSE on α, if the minimum of the function is at a large value of α, we wanted to determine the 95% confidence interval of the calculation of α. Twenty thousand normally distributed triplets of $I_1$, $I_2$, and $I_3$ were generated according to the means and standard deviations of the intensities corresponding to the two experimental setups presented in Figures 3A (α = 5.7) and 3B (α = 0.615). Then, α was determined from the simulated datasets, and a histogram was calculated from the 20,000 α values (Fig. 4). The histogram corresponding to α = 0.615 is somewhat narrower, but it has a long tail right of the peak. This results in an insignificant difference between the standard deviationss of the histograms (0.71 and 0.67 corresponding to α = 0.615 and α = 5.7, respectively). Similarly, the widths of the 95% confidence intervals of the calculations are not substantially different for the two cases (between −0.06 and 3.067 for α = 0.615; between 4.72 and 7.56 for α = 5.7). Equation 10 shows that the relative rather than the absolute error of α determines the error of FRET calculations. Therefore, we calculated the coefficient of variation (standard deviation divided by the mean) of the histograms that yielded 0.91 and 0.11, corresponding to α = 0.615 and α = 5.7, respectively. We concluded that the weak dependence of the MSE on α in the case of large α values does not deteriorate the reliability of FRET calculations.

### Correspondence Between Calculated and Experimentally Determined $R_F$-$R_I$ Plots

Using the values of α and the absorption ratio presented in Table 1, simulated $R_I$ and $R_F$ values were calculated according to equations 10 and 11, respectively, corresponding to a range of E values. The simulated $R_F$-$R_I$ curve and the experimentally determined three pairs of $R_F$-$R_I$ were plotted in the same graph (Fig. 5A), which can be regarded as a fit of equation 16 to the measurement. The correspondence between the fitted and the measured data was remarkably good.

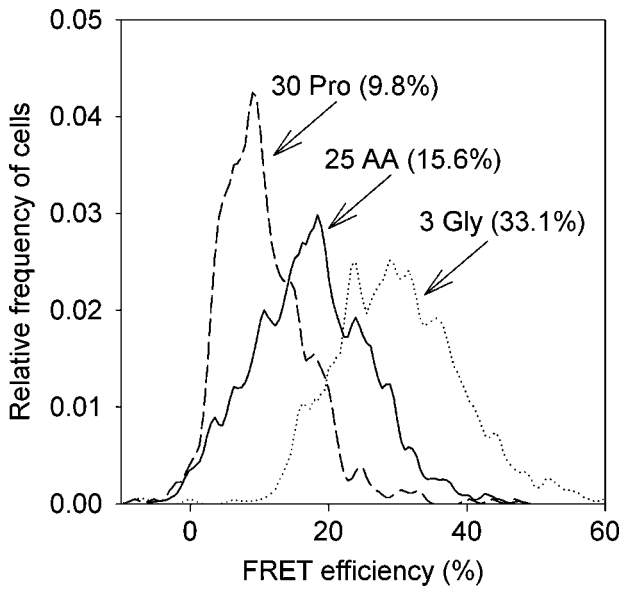


FIG. 2. Flow cytometric FRET histograms of three different CFP-YFP constructs. Yeast cells expressing constructs in which CFP and YFP were separated by three glycines, the 25 AA linker, or 30 prolines were analyzed by flow cytometry. The α value necessary for the calculation of FRET efficiency was determined, and FRET was determined on a cell-by-cell basis. The mean values of the three FRET histograms are displayed in parentheses.

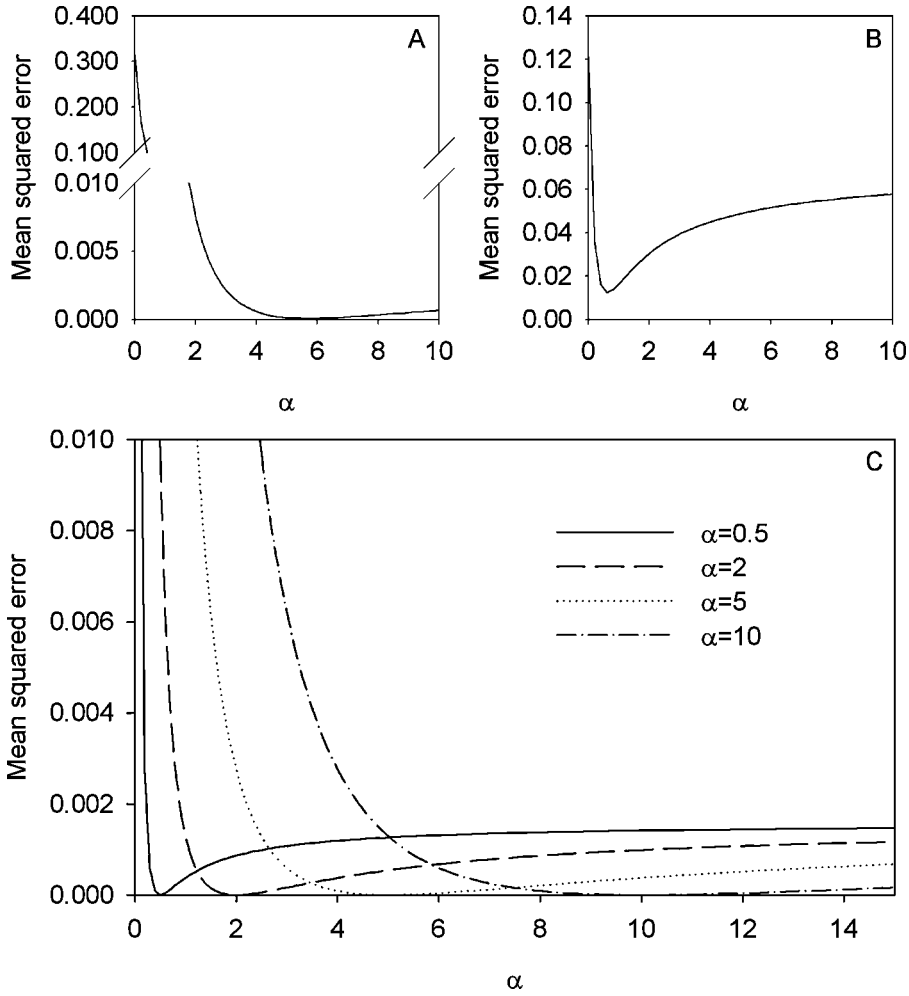


FIG. 3. Experimental and simulated mean squared errors of the minimization process as a function of α. **A, B:** Mean squared error of the minimization of equation 15 determined from flow cytometric data. $R_I$ and $R_F$ values displayed in Table 1 were substituted into equation 15, the minimization of which yielded α = 5.7. The mean squared error was plotted as a function of α (A). An identical calculation was carried out after measuring the same samples with flow cytometric data obtained with different instrument parameters yielding α = 0.615, and the mean squared error was plotted against α (B). **C:** Simulation of experimental data. Calculations were carried out by assuming that the FRET efficiencies of the measured samples were 5%, 15%, and 30% and the absorption ratio ($\varepsilon_D c_D/\varepsilon_A c_A$) was 5. $R_I$ and $R_F$ values were calculated for four different values of α (0.5, 2, 5, and 10), and the mean squared error was determined according to equation 19 and plotted as a function of α.

### Measurement of the Interaction Between p27-Kip1 and Cdk2

Cdk2 interacts with the inhibitor p27-Kip1 (30); therefore, we used them as a positive control to test the FRET system described above. A CFP-Kip1 chimera and a YFP-Cdk2 chimera were coexpressed in yeast cells and a FRET histogram was calculated from 10,000 cells (Fig. 6). The average FRET efficiency was calculated from the means of three such histograms and was 9 ± 2%. If YFP-Cdk2 was coexpressed with a random peptide fused to CFP, FRET was 1 ± 1%. Next, the CFP-Kip1 and YFP-Cdk2 coexpressing sample were subjected to sorting. Two sorting gates were defined as shown in Figures 7A and 7B. The gate in Figure 7A was created so that only cells expressing high levels of donor and acceptor are sorted and their relative expression ratio is not substantially different from 1. The second gate was placed on cells in which the intensity in the FRET channel was relatively high; therefore, an interaction between the two proteins can be expected. We must note that the separation between the excitation and emission wavelengths in the FRET channel (406 to 415 nm and 560/70 nm, respectively) were large; therefore, spectral overspill from direct donor or acceptor emission to the FRET channel was negligible. However, even in this case the intensity in the FRET channel is determined by the concentration of the donor and the FRET efficiency ($I_D \cdot E \cdot \alpha$), so offline FRET calculation was necessary to show that cells containing interacting proteins had been sorted. We first established that cells corresponding to the sorting gates were indeed sorted (Fig. 7C,D). Then, α was calculated using the method described in this reported, and FRET was determined on a cell-by-cell basis for the unsorted and sorted populations. This calculation clearly showed that the sorted population was enriched in cells containing interacting proteins (Fig. 7E).

## DISCUSSION

We have developed a novel flow cytometric method for the quantitative evaluation of the FRET efficiency between different VFPs on a cell-by-cell basis. A flow cytometric FRET calculation must involve a constant, designated α in the present report, that relates the fluorescence intensity of acceptor molecules to that of an equal number of excited donor molecules. The major merit of the present study is the elaboration of a novel method for the flow cytometric determination of α. In microscopy the determination of α can be based on the comparison of the inten-

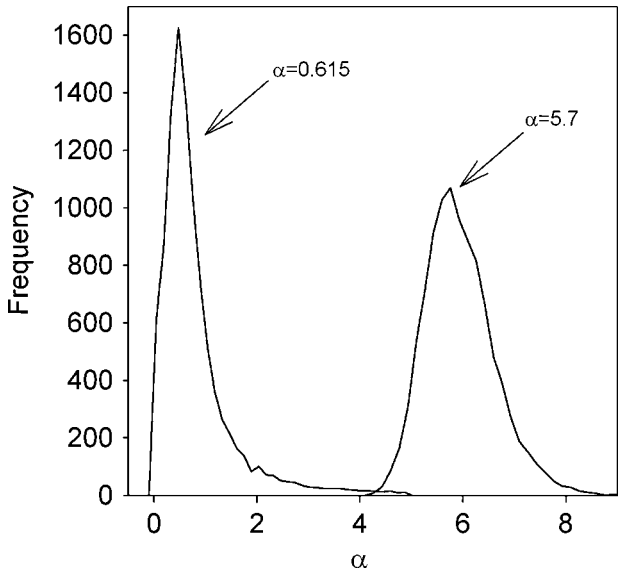


FIG. 4. Confidence interval of the determination of α. Means and standard deviations of parameters $I_1$, $I_2$, $I_3$, $S_1$, and $S_2$ corresponding to the flow cytometer settings yielding α = 5.7 and α = 0.615 were used to generate 20,000 normally distributed $I_1$, $I_2$, $I_3$, $S_1$, and $S_2$ variables from which $R_I$ and $R_F$ were calculated. Then, minimization of the mean squared error in equation 19 was carried out, and the distributions of the resultant α values were plotted. The 95% confidence intervals are 4.72 to 7.56 and 0.06 to 3.067 for the histograms corresponding to α = 5.7 and α = 0.615, respectively.

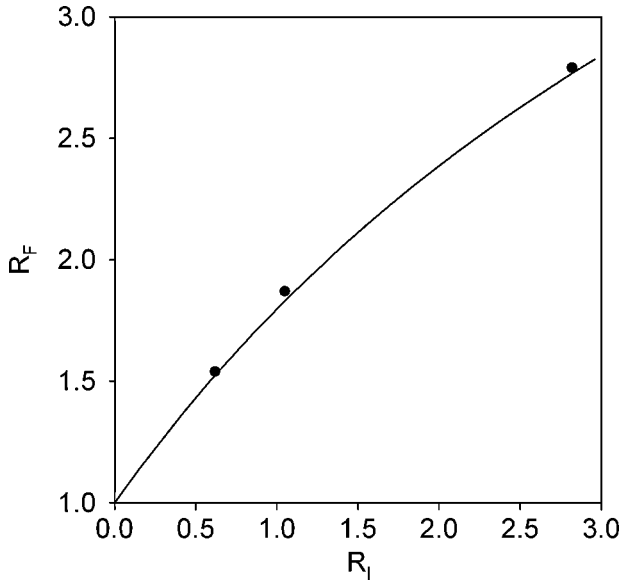


FIG. 5. Simulated and experimentally determined $R_I$ and $R_F$ values. The α value and the absorption ratio ($\varepsilon_D c_D/\varepsilon_A c_A$) determined from data in Table 1 were used to generate pairs of $R_I$ and $R_F$ values according to equations 10 and 11 by changing the FRET efficiency, and they were plotted together with the experimentally determined $R_I$ and $R_F$ values in Table 1.

sity lost on the acceptor side due to acceptor bleaching to the consequent increase in donor intensity due to release of quenching (13). Because photobleaching measurements are difficult to carry out in flow cytometry, the usual flow cytometric way to determine α is to compare the fluorescence intensity of an equal number of excited donor and acceptor molecules. When antibody- or ligand-labeled cells are used, this is usually done by separately labeling an equal number of epitopes with donor- and acceptor-tagged antibodies. Identical expression of two VFPs serving as a donor and acceptor pair can be achieved only if the two are part of a single protein. If there is no FRET between the donor and acceptor, α can be directly calculated using equation 18 provided the absorption ratio is known. We wanted to create such a CFP-YFP chimera by placing a linker consisting of 30 prolines between the two VFPs (31). If there had been no FRET between CFP and YFP in such a construct, it could have been used for the determination of α directly as described previously (17,18). However, initial measurements showed that FRETN and N-FRET parameters were not 0, indicating that FRET took place. The lack of correlation between the FRET efficiency and the expression level of the fusion construct indicated that intermolecular FRET did not play a role. Taking into account that the $R_o$ for the CFP-YFP pair is 4.9 nm (5), a FRET efficiency of 10% corresponds to a donor-acceptor separation distance of 7 nm. In a typical polyproline helix in an aqueous environment (polyproline helix type II), the helical rise per residue is 0.31 nm, yielding 9.3 nm for the separation between the N- and C-termini of the polyproline linker expected to result in a FRET efficiency of 2%. If the fluorophores are assumed to be at the end of the helix, the polyproline linker has to be significantly bent (with a curvature radius of 3.8 nm). Although polyproline helices can be distorted by asymmetric hydrogen bonding with surrounding water molecules, such a significant bending is unlikely. In contrast, CFP and YFP attached to the termini of the linker may

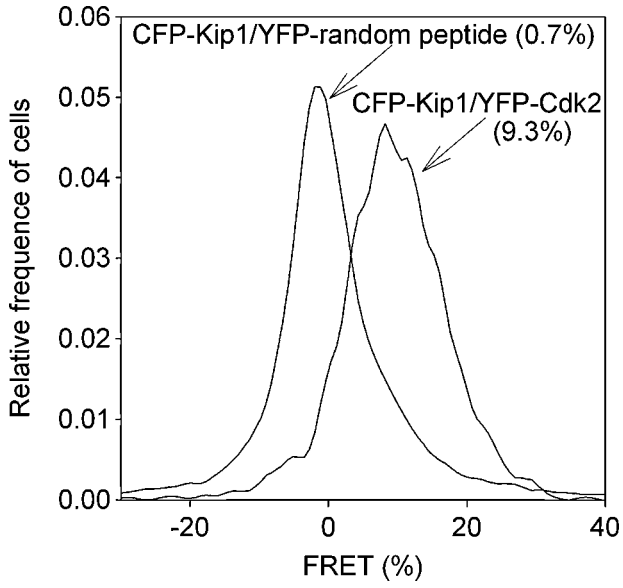


FIG. 6. Flow cytometric measurement of the interaction of p27-Kip1 with Cdk2 and a random peptide. Yeast cells expressing CFP-Kip1 and YFP-Cdk2 or CFP-Kip1 and YFP fused to a random peptide were analyzed by flow cytometry. FRET between CFP and YFP was quantitated and histograms of 10,000 cells were plotted. The mean FRET efficiencies are displayed in parentheses.

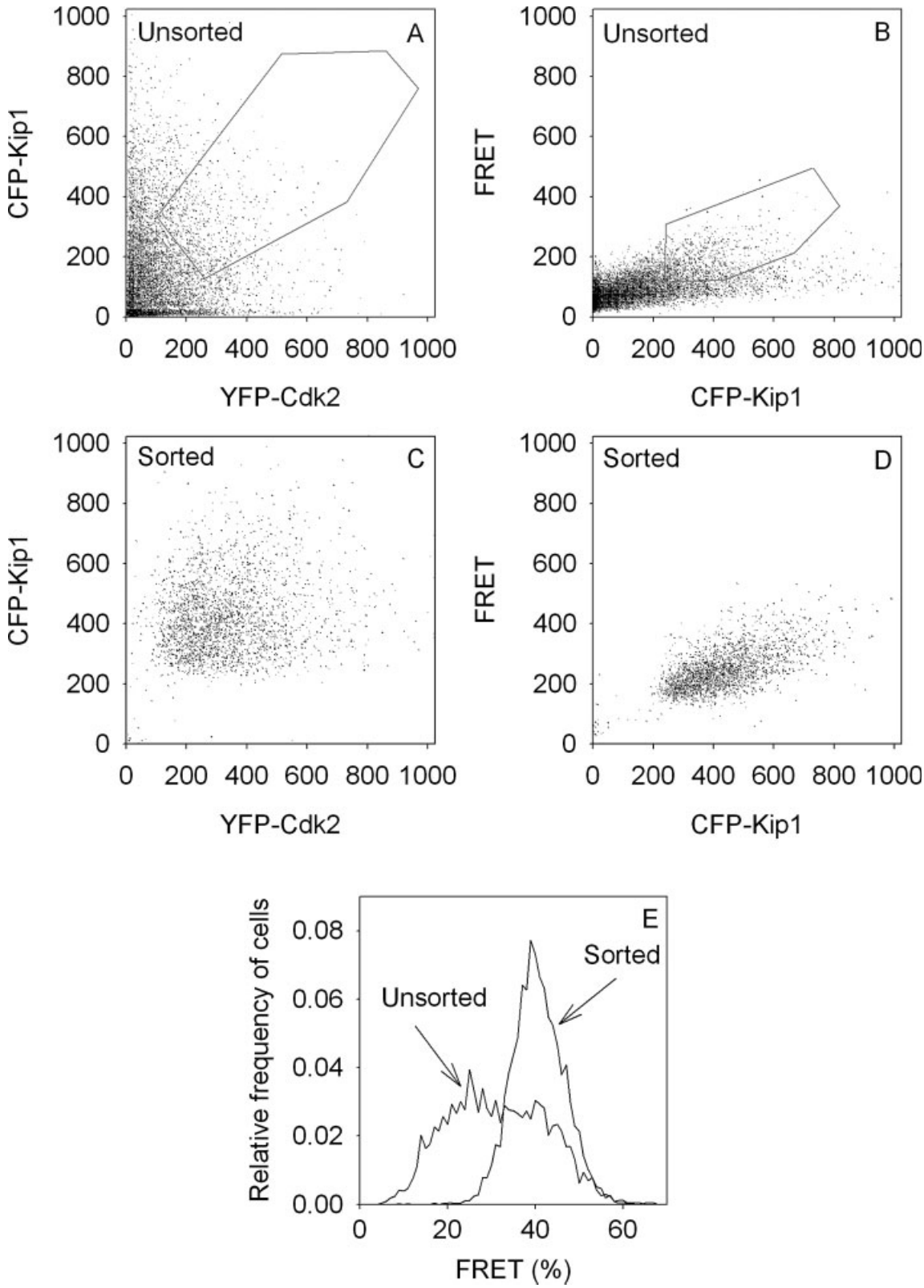


FIG. 7. Sorting of yeast cells based on the interaction between CFP-Kip1 and YFP-Cdk2. Yeast cells coexpressing CFP-Kip1 and YFP-Cdk2 were analyzed by flow cytometry, and fluorescence intensities in the donor (CFP-Kip1), acceptor (YFP-Cdk2), and FRET channels were measured. Numbers on the FRET axes in B and D are fluorescence intensity values and not calibrated FRET efficiencies as in E. **A, B:** Dot plots of unsorted cells. Cells expressing large amounts of CFP-Kip1 and YFP-Cdk2 at ~1:1 ratio displaying high fluorescence intensity in the FRET channel were sorted. The sorting gates are indicated in A and B. **C, D:** Two-parameter dot plots of sorted cells. **E:** FRET histograms were made by cell-by-cell FRET calculations carried out on unsorted and sorted cells.

swing toward each other, thus decreasing the separation distance between the fluorophores below the length of the linker. The presence of FRET in the CFP-30Pro-YFP sample was the major motive to elaborate the method for the determination of α described in this report, which does not rely on the lack of FRET in the calibration samples or knowledge of the absorption ratio.

Our method requires at least two samples with different FRET efficiencies expressing donor-acceptor chimeras strictly generating a donor to acceptor ratio of 1. The reliability of the method is significantly enhanced if there are at least three calibration samples. FRET is calculated using two different approaches (equations 10 and 14) that yield two FRET-related ratios ($R_I$ and $R_F$). The relation between $R_I$ and $R_F$ is determined by the absorption ratio and α according to equations 16 and 17. These equations can be used to derive the absorption ratio and α in a single step by fitting equation 16 or 17 to the $R_F$-$R_I$ or $1/(R_F - 1) - 1/R_I$ plot, respectively. From a practical point of view, the number of calibration samples is usually small; in our case it was three, so fitting two parameters to three measurement data points is prone to errors. If there were a much larger number of calibration samples, fitting of equation 16 or 17 could be reliably used, but the requirement for a larger set of calibration samples would make the method more costly and laborious. Our method eliminates this drawback by creating a ratio norm whose squared sum can be minimized by changning only α (equation 15) and then finding the absorption ratio by linear regression (equation 11). We verified our flow cytometric method by determining the FRET efficiency of the CFP-YFP construct containing a trypsin-sensitive linker by trypsin digestion, which induces the separation of the donor and the acceptor and a concomitant de-quenching of the donor (26). This measurement yielded a FRET value not significantly different from our flow cytometric determination.

The dependence of the MSE on α was relatively weak if α was large, especially above the minimum (equation 19, Fig. 3). However, the 95% confidence interval of α was not substantially different between small and large values of α due to presence of a tail in the frequency histogram of calculated α values above the optimal value of α if α was small (Fig. 4).

We have successfully applied the described approach for the CFP-YFP pair, but we could not achieve a reliable determination of α with the BFP-GFP donor-acceptor pair. The major cause of the failure must have been the low fluorescence quantum yield and high bleaching rate of BFP (32) and the high level of autofluorescence in this spectral region. Low donor intensity severely increases the error of equation 10 (18). In addition, equation 8 shows that a low donor fluorescence quantum yield increases α, resulting in a weak dependence of the MSE on α.

Finding interaction partners of a protein is a frequent problem in the post-genomic era. Currently, yeast two-hybrid (33,34) and fluorescence complementation (35) techniques are used to find interaction partners for a protein of interest. Both approaches are based on the reconstitution of some kind of an activity (e.g., transcription, fluorescence) after two halves of a protein are brought together by the association of two interacting proteins the two fragments are genetically fused to. A lingering question about these methods is whether an interaction is driven by the two halves of the transcription factor (yeast two-hybrid) or VFP (fluorescence complementation) or by the proteins they are fused to. We demonstrated that cells can be sorted based on FRET. Sorting was done based on the intensity in the FRET channel, which is determined not only by FRET. Faster electronics can perform online FRET calculations according to equation 10, making sorting based on accurate FRET values possible. If a bait is fused to CFP and a library of YFP-fused proteins is generated, then FRET can be used as a marker for the interaction and cells can be sorted accordingly (36). Similarly to the split ubiquitin system (33), our approach is exquisitely suited for the study of membrane protein interactions, an area that was not amenable to yeast two-hybrid experiments.

The deficiency of calculating fluorescence intensities in the FRET channel instead of real FRET efficiencies is demonstrated by a recently published report in which the investigators examined the interaction between CFP- and YFP-tagged proteins in live yeast cells based on measuring FRET intensities (9). Due to the sensitivity of FRET intensity for the expression level of VFPs, the distinction between "significant" and "nonsignificant" FRET intensity is rather subjective, probably resulting in an underestimation of the fraction of cells showing FRET, as the investigators acknowledge. These investigators (9) also suggested using FRET measurements to screen VFP-tagged proteins for interactions. We believe that this could be accomplished using our quantitative approach in a much more sensitive way.

We have developed a method for the quantitation of FRET between VFPs in flow cytometry. Our approach eliminates the pitfalls of calculating FRET indices instead of FRET efficiency. We have demonstrated the successful application of the method for the CFP-YFP donor-acceptor pair. Quantitative FRET measurements have the potential to identify and characterize molecular interactions in their native environment more accurately than currently used molecular biological techniques.

## LITERATURE CITED

1. Stryer L. Fluorescence energy transfer as a spectroscopic ruler. Annu Rev Biochem 1978;47:819–846.
2. Dexter DL. A theory of sensitized luminescence in solids. J Chem Phys 1953;21:836–850.
3. Förster T. Energiewanderung und Fluoreszenz. Naturwissenschaften 1946;6:166–175.
4. Clegg RM. Fluorescence resonance energy transfer. Curr Opin Biotechnol 1995;6:103–110.
5. Patterson GH, Piston DW, Barisas BG. Forster distances between green fluorescent protein pairs. Anal Biochem 2000;284:438–440.
6. Jares-Erijman EA, Jovin TM. FRET imaging. Nat Biotechnol 2003;21:1387–1395.
7. Szöllsi J, Damjanovich S, Mátyus L. Application of fluorescence resonance energy transfer in the clinical laboratory: routine and research. Cytometry 1998;34:159–179.

8. Szöllsi J, Nagy P, Sebestyén Z, Damjanovich S, Park JW, Mátyus L. Applications of fluorescence resonance energy transfer for mapping biological membranes. Rev Mol Biotechnol 2002;82:251–266.
9. Dye BT, Schell K, Miller DJ, Ahlquist P. Detecting protein-protein interaction in live yeast by flow cytometry. Cytometry A 2005;63A:77–86.
10. Berney C, Danuser G. FRET or no FRET: a quantitative comparison. Biophys J 2003;84:3992–4010.
11. Gordon GW, Berry G, Liang XH, Levine B, Herman B. Quantitative fluorescence resonance energy transfer measurements using fluorescence microscopy. Biophys J 1998;74:2702–2713.
12. Xia Z, Liu Y. Reliable and global measurement of fluorescence resonance energy transfer using fluorescence microscopes. Biophys J 2001;81:2395–2402.
13. Zal T, Gascoigne NR. Photobleaching-corrected FRET efficiency imaging of live cells. Biophys J 2004;86:3923–3939.
14. Rocheleau JV, Edidin M, Piston DW. Intrasequence GFP in class I MHC molecules, a rigid probe for fluorescence anisotropy measurements of the membrane environment. Biophys J 2003;84:4078–4086.
15. Lidke DS, Nagy P, Barisas BG, Heintzmann R, Post JN, Lidke KA, Clayton AH, Arndt-Jovin DJ, Jovin TM. Imaging molecular interactions in cells by dynamic and static fluorescence anisotropy (rFLIM and emFRET). Biochem Soc Trans 2003;31:1020–1027.
16. Squire A, Verveer PJ, Rocks O, Bastiaens PI. Red-edge anisotropy microscopy enables dynamic imaging of homo-FRET between green fluorescent proteins in cells. J Struct Biol 2004;147:62–69.
17. Szöllsi J, Trón L, Damjanovich S, Helliwell SH, Arndt Jovin D, Jovin TM. Fluorescence energy transfer measurements on cell surfaces: a critical comparison of steady-state fluorimetric and flow cytometric methods. Cytometry 1984;5:210–216.
18. Trón L, Szöllsi J, Damjanovich S, Helliwell SH, Arndt Jovin DJ, Jovin TM. Flow cytometric measurement of fluorescence resonance energy transfer on cell surfaces. Quantitative evaluation of the transfer efficiency on a cell-by-cell basis. Biophys J 1984;45:939–946.
19. Nagy P, Vámosi G, Bodnár A, Lockett SJ, Szöllsi J. Intensity-based energy transfer measurements in digital imaging microscopy. Eur Biophys J 1998;27:377–389.
20. Bastiaens PI, Majoul IV, Verveer PJ, Soling HD, Jovin TM. Imaging the intracellular trafficking and state of the AB5 quaternary structure of cholera toxin. EMBO J 1996;15:4246–4253.
21. Karpova TS, Baumann CT, He L, Wu X, Grammer A, Lipsky P, Hager GL, McNally JG. Fluorescence resonance energy transfer from cyan to yellow fluorescent protein detected by acceptor photobleaching using confocal microscopy and a single laser. J Microsc 2003;209:56–70.
22. Braun M.Fluoreszenz-optimierte Detektion heterologer Protein-Protein Interaktionen in Saccharomyces cerevisiae als Alternative zur Yeast Two Hybrid Methode (PhD dissertation). Tübingen: Faculty of Chemistry and Pharmacy, Eberhard Karls University; 2001.
23. Cormack BP, Bertram G, Egerton M, Gow NA, Falkow S, Brown AJ. Yeast-enhanced green fluorescent protein (yEGFP): a reporter of gene expression in *Candida albicans*. Microbiology 1997;143:303–311.
24. Heim R, Prasher DC, Tsien RY. Wavelength mutations and posttranslational autoxidation of green fluorescent protein. Proc Natl Acad Sci USA 1994;91:12501–12504.
25. Heim R, Cubitt AB, Tsien RY. Improved green fluorescence. Nature 1995;373:663–664.
26. Heim R, Tsien RY. Engineering green fluorescent protein for improved brightness, longer wavelengths and fluorescence resonance energy transfer. Curr Biol 1996;6:178–182.
27. Kahana JA, Schnapp BJ, Silver PA. Kinetics of spindle pole body separation in budding yeast. Proc Natl Acad Sci USA 1995;92:9707–9711.
28. Yang F, Moss LG, Phillips GN, Jr. The molecular structure of green fluorescent protein. Nat Biotechnol 1996;14:1246–1251.
29. Zernicka-Goetz M, Pines J, McLean HS, Dixon JP, Siemering KR, Haseloff J, Evans MJ. Following cell fate in the living mouse embryo. Development 1997;124:1133–1137.
30. Olashaw N, Pledger WJ. Paradigms of growth control: relation to Cdk activation. Sci STKE 2002;2002:RE7.
31. Stryer L, Haugland RP. Energy transfer: a spectroscopic ruler. Proc Natl Acad Sci USA 1967;58:719–726.
32. Patterson G, Day RN, Piston D. Fluorescent protein spectra. J Cell Sci 2001;114:837–838.
33. Thaminy S, Miller J, Stagljar I. The split-ubiquitin membrane-based yeast two-hybrid system. Methods Mol Biol 2004;261:297–312.
34. Miller J, Stagljar I. Using the yeast two-hybrid system to identify interacting proteins. Methods Mol Biol 2004;261:247–262.
35. Hu CD, Kerppola TK. Simultaneous visualization of multiple protein interactions in living cells using multicolor fluorescence complementation analysis. Nat Biotechnol 2003;21:539–545.
36. Paysan J, Herlitze S, Antz C, Ruppersberg JP. Verfahren zur Identifizierung von Wechselwirkungen zwischen Proteinen und Peptiden durch FRET. Germany patentDE19737562; 1997.